

## Detection probability and density estimation of fin whales by a Seaglider

Selene Fregosi, Danielle V. Harris, Haruyoshi Matsumoto, et al.

Citation: *The Journal of the Acoustical Society of America* **152**, 2277 (2022); doi: 10.1121/10.0014793

View online: <https://doi.org/10.1121/10.0014793>

View Table of Contents: <https://asa.scitation.org/toc/jas/152/4>

Published by the [Acoustical Society of America](#)

---

### ARTICLES YOU MAY BE INTERESTED IN

[Source separation with an acoustic vector sensor for terrestrial bioacoustics](#)

*The Journal of the Acoustical Society of America* **152**, 1123 (2022); <https://doi.org/10.1121/10.0013505>

[A wave glider-based, towed hydrophone array system for autonomous, real-time, passive acoustic marine mammal monitoring](#)

*The Journal of the Acoustical Society of America* **152**, 1814 (2022); <https://doi.org/10.1121/10.0014169>

[A survey of sound source localization with deep learning methods](#)

*The Journal of the Acoustical Society of America* **152**, 107 (2022); <https://doi.org/10.1121/10.0011809>

[Shallow-water waveguide acoustic analysis in a fluctuating environment](#)

*The Journal of the Acoustical Society of America* **152**, 1252 (2022); <https://doi.org/10.1121/10.0013831>

[Near real-time detection of low-frequency baleen whale calls from an autonomous surface vehicle: Implementation, evaluation, and remaining challenges](#)

*The Journal of the Acoustical Society of America* **149**, 2950 (2021); <https://doi.org/10.1121/10.0004817>

[Acoustic detection range of right whale upcalls identified in near-real time from a moored buoy and a Slocum glider](#)

*The Journal of the Acoustical Society of America* **151**, 2558 (2022); <https://doi.org/10.1121/10.0010124>

---




**Advance your science and career  
as a member of the**

**ACOUSTICAL SOCIETY OF AMERICA**

LEARN MORE



## Detection probability and density estimation of fin whales by a Seaglider

Selene Fregosi,<sup>1,a)</sup>  Danielle V. Harris,<sup>2</sup>  Haruyoshi Matsumoto,<sup>1</sup> David K. Mellinger,<sup>1</sup>  Stephen W. Martin,<sup>3</sup> Brian Matsuyama,<sup>3</sup> Jay Barlow,<sup>4</sup>  and Holger Klinck<sup>5,b)</sup> 

<sup>1</sup>Cooperative Institute for Marine Ecosystem and Resources Studies, Oregon State University and National Oceanic and Atmospheric Administration Pacific Marine Environmental Laboratory, 2030 Southeast Marine Science Drive, Newport, Oregon 97365, USA

<sup>2</sup>Centre for Research into Ecological and Environmental Modelling, University of St Andrews, St Andrews, Fife KY16 9LZ, United Kingdom

<sup>3</sup>National Marine Mammal Foundation, San Diego, California 92106, USA

<sup>4</sup>Marine Mammal and Turtle Division, Southwest Fisheries Science Center, National Oceanic and Atmospheric Administration National Marine Fisheries Service, La Jolla, California 92037, USA

<sup>5</sup>K. Lisa Yang Center for Conservation Bioacoustics, Cornell Lab of Ornithology, Cornell University, Ithaca, New York 14850, USA

### ABSTRACT:

A single-hydrophone ocean glider was deployed within a cabled hydrophone array to demonstrate a framework for estimating population density of fin whales (*Balaenoptera physalus*) from a passive acoustic glider. The array was used to estimate tracks of acoustically active whales. These tracks became detection trials to model the detection function for glider-recorded 360-s windows containing fin whale 20-Hz pulses using a generalized additive model. Detection probability was dependent on both horizontal distance and low-frequency glider flow noise. At the median 40-Hz spectral level of 97 dB re 1  $\mu\text{Pa}^2/\text{Hz}$ , detection probability was near one at horizontal distance zero with an effective detection radius of 17.1 km [coefficient of variation (CV) = 0.13]. Using estimates of acoustic availability and acoustically active group size from tagged and tracked fin whales, respectively, density of fin whales was estimated as 1.8 whales per 1000 km<sup>2</sup> (CV = 0.55). A plot sampling density estimate for the same area and time, estimated from array data alone, was 1.3 whales per 1000 km<sup>2</sup> (CV = 0.51). While the presented density estimates are from a small demonstration experiment and should be used with caution, the framework presented here advances our understanding of the potential use of gliders for cetacean density estimation. © 2022 Acoustical Society of America.

<https://doi.org/10.1121/10.0014793>

(Received 10 October 2021; revised 30 June 2022; accepted 23 September 2022; published online 21 October 2022)

[Editor: Klaus Lucke]

Pages: 2277–2291

### I. INTRODUCTION

Estimated population density, or the estimated number of animals present per unit area, is a useful metric for identifying potential changes in cetacean populations and is necessary for successful management and conservation. Density can be estimated from actually counting animals or, alternatively, from some indicator of an animal's presence, called a cue, such as visual observations of whale blows or recorded acoustic signals (Buckland, 2006; Buckland *et al.*, 2015; Marques *et al.*, 2013). Estimating density from acoustic data is particularly effective for cetaceans; acoustic cues may be more detectable than visual cues because they propagate over longer ranges and can be readily detected by autonomous platforms capable of more persistent monitoring than visual surveys (Barlow *et al.*, 2013; Marques *et al.*, 2013).

One of the challenges for passive acoustic density estimation (and animal density estimation in general) is to quantify the total area monitored and the probability of

detecting target animals within that area. Generally, the likelihood an acoustic cue, hereafter called an acoustic event, is detected decreases with its distance from the hydrophone, similar to visual surveys where animals are typically more difficult to see further from the observer. Additionally, animals near the hydrophone may not be detected because they may not be producing cues. An estimate of animal density, from either visual or acoustic data, requires an estimate of the detection function,  $g(y)$ , which models the probability of detection of an acoustic event as a function of the horizontal distance,  $y$ , from the hydrophone (Buckland *et al.*, 2001). For cetacean species that can be producing acoustic events at depth or for hydrophones that can be located in the water column or on the sea floor, horizontal distance is the distance between the hydrophone and the location where the acoustic event is produced, projected onto a horizontal plane. The detection function is then used to estimate the effective survey area, which can be used to convert the number of detected acoustic events to an estimate of the density of acoustic events. To go from density of acoustic events to density of animals, additional pieces of information related to acoustic behavior, such as an estimate of the rate at which

<sup>a)</sup>Electronic mail: selene.fregosi@gmail.com

<sup>b)</sup>Also at: Marine Mammal Institute, Department of Fisheries Wildlife and Conservation, Oregon State University, Newport, OR 97365, USA.

the population produces the acoustic event of interest (often referred to as the cue production rate or call production rate) or the availability of acoustic events for detection within a given time period (acoustic availability), are required. If an appropriate estimate of the relevant acoustic behavior parameter is available, animal density can be estimated from acoustic event density (Buckland *et al.*, 2001; Marques *et al.*, 2013).

Distance sampling can be used to estimate the detection function and has been used to estimate density of a variety of cetaceans through both visual and acoustic surveys (e.g., Barlow and Taylor, 2005; Gerrodette *et al.*, 2011; Marques *et al.*, 2011; McDonald and Fox, 1999; Norris *et al.*, 2017). Acoustic distance sampling can take the form of line-transect distance sampling, using a vessel towing a hydrophone array, or fixed point-transect distance sampling, in which a stationary hydrophone is the survey point (Harris *et al.*, 2013). In either case, the number of acoustic events detected is quantified, the distance to each detected event is estimated [either using time difference of arrival (TDOA) information or auxiliary methods such as simultaneous tag deployments, visual surveys, or propagation modeling], and the distribution of these distances is used to estimate the detection function. Distance sampling requires that animals be detected at their initial location (i.e., there is no animal movement) so that density estimates are not biased by animals moving into the survey area or by moving toward or away from the hydrophone (either randomly or in response to the survey platform) (Buckland *et al.*, 2001; Glennie *et al.*, 2015). For a vessel-based line-transect survey, the vessel is typically moving sufficiently quickly (faster than the animals) to ensure that animal movement relative to the ship is trivially small. For point-transect sampling, animal presence in a short duration time window, otherwise known as a “snapshot,” can be used as the acoustic event of interest to overcome potential animal movement that could bias the density estimate (Buckland, 2006). The length of the snapshot window needs to be defined for the target species, such that animal movement within the snapshot window can be assumed to be negligible relative to the detection distances. Distance sampling also assumes that the detection probability at zero horizontal distance from the survey trackline or point [symbolized as  $g(0)$ ] is either certain (equal to 1) or is known and that distances to detections are measured accurately. These assumptions make it difficult to apply distance sampling to some passive acoustic surveys, including those from mobile, autonomous platforms.

Autonomous underwater vehicles, such as gliders, have proven to be effective survey platforms for passive acoustic monitoring (PAM) of cetaceans. Gliders provide several advantages over traditional stationary or vessel-based methods [see Verfuss *et al.* (2019) for a review of autonomous systems]. The primary advantage of gliders is increased spatial coverage compared to a stationary sensor and increased temporal coverage compared to a vessel-based survey. Gliders have been used to acoustically detect and survey for a variety of cetacean species (e.g., Baumgartner *et al.*, 2013;

Cauchy *et al.*, 2020; Fregosi *et al.*, 2020a; Klinck *et al.*, 2016; Kowarski *et al.*, 2020; Silva *et al.*, 2019), and there is an interest in using these systems to estimate cetacean population densities (Gkikopoulou, 2018; Harris *et al.*, 2017; Küsel *et al.*, 2017; Marques *et al.*, 2013). However, applying passive acoustic density estimation methods to glider data is not straightforward because of the glider’s slow movement, the combination of horizontal and vertical glider movement, low-frequency flow noise generated through glider movement, and the glider’s relatively small size, which limits the available aperture for multiple acoustic sensors. Each of these considerations is discussed in more detail below.

Slow glider movement may violate the first distance sampling assumption that animals are detected at their initial location. Typical horizontal glider speeds (25 cm/s; Rudnick *et al.*, 2004) are slower than typical marine mammal movement (1–2 m/s; Sato *et al.*, 2007). This assumption can be overcome by using a snapshot approach, where the glider track is divided into temporal snapshots and each snapshot is then treated as a point-transect sample, rather than treating the glider’s path as a continuous survey transect as used in Barlow *et al.* (2021) for drifting recorders. The appropriate snapshot duration is short enough that animal movement is negligible in relation to the detection distances but long enough that reliable detection and classification of the target acoustic event are still possible.

The three-dimensional (3D) movement of the glider presents unique considerations for PAM and density estimation (Marques *et al.*, 2013). The glider moves up and down in the water column, which turns the traditionally two-dimensional (2D) detection probability function into a 3D problem (Buckland *et al.*, 2015). Sound speed underwater varies with water depth, temperature, and salinity; underwater sound propagation is affected by differences in the sound speed profile (Urick, 1983). Because the glider is moving both horizontally and vertically, the detection probability may change over the course of a dive cycle and/or over a survey duration (Gkikopoulou, 2018; Harris *et al.*, 2017). Additionally, there is evidence that the glider-generated low-frequency flow noise can vary during a survey, which would change the detection probability (Fregosi *et al.*, 2020b). While detection probability from a moving platform is inherently complicated, distance sampling methods can accommodate heterogeneity in detection probability (Buckland *et al.*, 2001). The effect of variables such as ambient or flow noise levels, glider depth, and location within the survey on detection probability can be investigated by including covariates in the detection function.

However, the inability to directly measure distances to detected events is a major difference of glider surveys compared to other PAM density estimation applications. Accurately estimating the distances to detected acoustic events is difficult using data from a single glider alone as gliders are typically single-hydrophone systems (Verfuss *et al.*, 2019). Single-hydrophone systems typically do not provide information on the bearing and range to the sound source; at least three sensors are traditionally needed to

estimate range of a sound source using TDOA methods. Küsel *et al.* (2017) instrumented a glider with two hydrophones, one on each wing, and were able to estimate bearing angles and generate animal tracks for sperm whales (*Physeter macrocephalus*). The authors demonstrated that multi-hydrophone systems may allow for direct distance measurements in the future; however, the hydrophone spacing (only 1 m along the wingspan of a Seaglider) and method used would not work well for low-frequency (<100 Hz) baleen whale vocalizations, which have signal wavelengths longer than 15 m (Küsel *et al.*, 2017).

If range to detected acoustic events cannot be measured directly, as is the case with most glider systems, the necessary detection probability can be estimated using auxiliary data (Marques *et al.*, 2013). Animal locations can be measured from additional instruments, and a set of detection “trials” can be assembled. For each trial, whether the located animal was detected or not by the acoustic system can be used to model a detection function. For example, Kyhn *et al.* (2012) conducted a visual survey at the same time and place as an acoustic survey. Shore-based observations provided known animal locations in relation to the hydrophones, so a detection function could be estimated for the acoustic data alone (Kyhn *et al.*, 2012). Marques *et al.* (2009) estimated a detection function for bottom-moored hydrophones using a similar trial-based approach. Animal-borne tags (e.g., DTAGs; Johnson and Tyack, 2003) provided animal location and vocal activity information, which was then used to quantify ranges at which the bottom-moored hydrophone did or did not detect echolocation clicks (Marques *et al.*, 2009).

We conducted an experiment to determine the feasibility of estimating fin whale (*Balaenoptera physalus*) density using a single-hydrophone passive acoustic glider survey. The primary objectives were to (1) assess the ability to estimate the detection probability of acoustic events produced by fin whales from an autonomous underwater glider and (2) develop a framework for estimating both the density of acoustic events and density of fin whales from glider-collected acoustic data. We used a trial-based approach, leveraging an extensive cabled hydrophone array operated by the U.S. Navy in the Southern California Bight that is capable of tracking baleen whales to provide known animal locations and to provide a second density estimate for comparison. The acoustic event of interest is the presence or absence of fin whale 20-Hz pulses within a snapshot. Glider noise levels in a frequency band adjacent to fin whale 20-Hz pulses (40 Hz single band noise levels) are included as a covariate in the detection function.

Fin whales were selected as the focal species for several reasons. Fin whale acoustic behavior is relatively well documented, which is necessary for estimating animal density from acoustic event density. Fin whales produce stereotyped low-frequency acoustic signals. The most common signal type is the 20-Hz pulse—a ~1 s duration pulsed downswEEP from 30 to 20 Hz that is found worldwide and produced year-round in Southern California (Širović *et al.*, 2013;

Thompson *et al.*, 1992; Watkins, 1981; Watkins *et al.*, 1987). Typical calling depths are 15–20 m (Stimpert *et al.*, 2015). Stereotyped, regular, and long-duration sequences of 20-Hz pulses form fin whale song, which has only been documented to be produced by males and is hypothesized to function in mate attraction (Croll *et al.*, 2002). Several song types, differing by the timing between subsequent pulses (interpulse interval), are known to occur in Southern California, and the doublet type (containing two distinct interpulse intervals) is most common (Oleson *et al.*, 2014; Širović *et al.*, 2017). Irregular bouts and call-counter call patterns of 20-Hz pulses have also been recorded, so this signal may also function as a contact call or in social interactions (McDonald *et al.*, 1995; Stimpert *et al.*, 2015; Watkins *et al.*, 1987). Fin whales take 1–20 min “rests” (average 2 min) within pulse bouts (Watkins *et al.*, 1987). In the North Pacific, fin whales also produce a higher-frequency downswEEP from 75 to 40 Hz, which is recorded mostly in the summer and is thought to be associated with feeding (Širović *et al.*, 2013; Watkins, 1981). We focused only on the 20-Hz pulse for this study. Fin whale 20-Hz pulses were plentiful in the recorded data, and they provide an example of a high source level, low-frequency baleen whale signal that can be detected over tens of kilometers (Širović *et al.*, 2007; Širović *et al.*, 2015; Stafford *et al.*, 2007). Finally, fin whales are of conservation concern because they are present in Southern California year-round (e.g., Barlow and Forney, 2007; Campbell *et al.*, 2015; Širović *et al.*, 2015), feeding and breeding in an area with high levels of anthropogenic activities, including commercial shipping, military exercises, and recreational fishing and boating activity, and are still considered endangered as a result of depletion by historical whaling (Carretta *et al.*, 2020).

## II. METHODS

### A. Acoustic data collection and analysis

A passive acoustic Seaglider (commercially available from Huntington-Ingalls Industries, Lynnwood, WA), equipped with a single hydrophone, was deployed for 2 weeks in the San Nicolas Basin of the Southern California Bight. The Seaglider (SG158) surveyed in the vicinity of the Southern California Offshore Range (SCORE), a U.S. Navy operated array of bottom-mounted, cabled hydrophones (Fig. 1). The Seaglider was deployed on 22 December 2015 on the north side of SCORE and surveyed the area in evenly spaced (~10 km) transects, continuously diving between the sea surface and 1000 m depth. It was recovered southeast of SCORE on 4 January 2016 (Fig. 1).

The Seaglider recorded passive acoustic data with the Wideband Intelligent Signal Processor and Recorder (WISPR; Embedded Ocean Systems, Inc., Boston, MA). Recordings were made continuously primarily when the glider was below 200 m depth [except for a few dives with shallower recordings made at the start of the survey; see Fregosi *et al.* (2020b) for additional detail] via a single



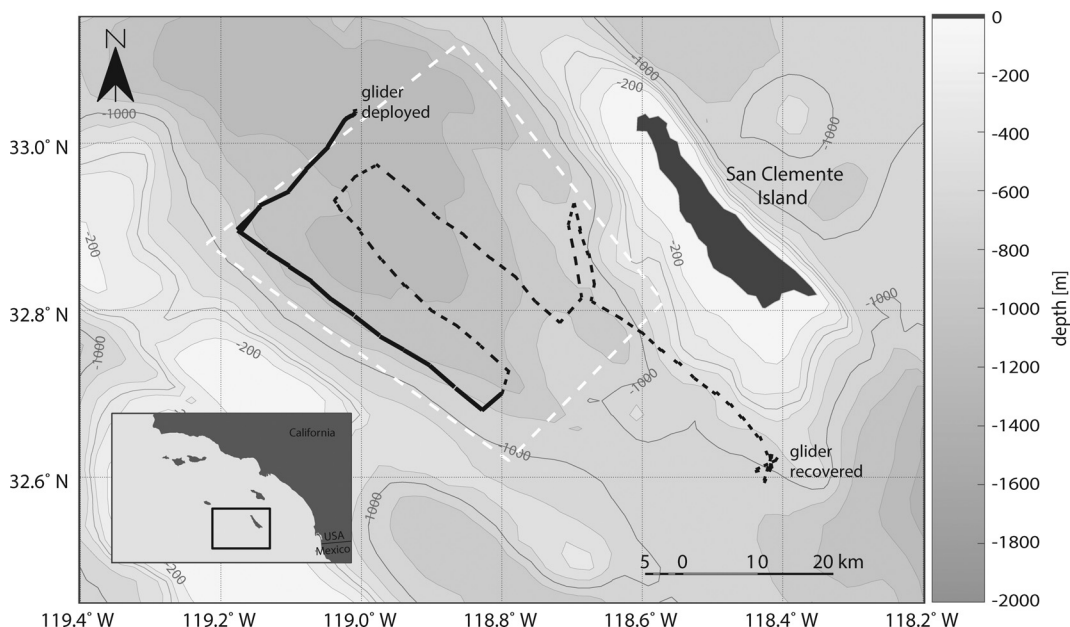


FIG. 1. Map of Seaglider, SG158, survey path (black line) and the general location of the SCORE hydrophone array (white dashed box). The glider was deployed to the northwest of the SCORE array and recovered south of San Clemente Island. The solid black line indicates the glider survey period that was analyzed for this experiment; the dashed black line is the remainder of the survey. Bathymetry is shown in 200 m contours from  $-200$  m (white) to  $-2000$  m (darkest gray). Bathymetry data are from the National Oceanic and Atmospheric Administration's (NOAA's) National Centers for Environmental Information (Amante and Eakins, 2009).

omni-directional hydrophone (HTI-92-WB, High Tech Inc., Gulfport, MS; sensitivity:  $-175$  dB re  $1 \text{ V}/\mu\text{Pa} \pm 3$  dB frequency response from 2 Hz to 50 kHz). The hydrophone was mounted inside the hull of the rear third of the glider, near the external buoyancy bladder. The system recorded at a 125 kHz sampling rate with 16-bit resolution [0–5 V differential analog-to-digital converter (ADC) input range] and was compressed using the Free Lossless Audio Codec (FLAC). Prior to digitization, a frequency-dependent gain curve approximately matching the inverse of a typical deep-water ambient noise spectrum was applied (see Matsumoto *et al.*, 2015) to maximize dynamic range across the recorded frequency spectrum. Overall analog system sensitivity at 20 Hz was  $-158$  dB re  $1 \text{ V}/\mu\text{Pa}$ . After the recovery of the glider, data were downsampled to 1 kHz to facilitate the analysis of low-frequency fin whale pulses. The local sound speed profile, measured by the glider-mounted conductivity-temperature-depth (CTD) sensor (Sea-Bird Electronics, Inc., Bellevue, WA) is provided in supplementary Fig. 1.<sup>1</sup>

Glider noise levels at 40 Hz [single Hz power spectral density (PSD) level; calculated with a 10-s Hann window and 0% overlap] were calculated for every minute of recording, as described in Fregosi *et al.* (2020b). A frequency of 40 Hz was chosen because it is adjacent to, but exclusive of, the frequency range of a fin whale 20-Hz pulse and therefore adequately captures changes in flow noise without including fin whale pulse energy. The lowest 40-Hz PSD level per minute was extracted to represent noise level in each minute. By selecting the lowest PSD level per minute, any transient sounds, such as glider motor noise, were excluded while still characterizing the flow noise, which did not change over 1 min. All 40 Hz noise levels reported hereafter are PSD levels in dB re  $1 \mu\text{Pa}^2/\text{Hz}$ .

While the glider was deployed, acoustic data from an array of bottom-moored hydrophones at SCORE were archived using the Marine Mammal Monitoring on Navy Ranges (M3R) system (Jarvis *et al.*, 2014). The SCORE hydrophones are located off the western shore of San Clemente Island in the Southern California Bight. They are moored at 800–1800 m water depth in a grid with approximately 4 km spacing between hydrophones (Fig. 1). The subset of 79 hydrophones used in this study recorded data at a 96 kHz sampling rate and 16-bit resolution. The standard configuration at SCORE applies a 50-Hz high pass filter to recorded data at the hydrophone locations, providing a frequency response range of  $\sim 50$  Hz to 48 kHz, but acoustic data are usable down to 20 Hz (Jarvis *et al.*, 2014; Moretti *et al.*, 2016). The M3R system is capable of recording, detecting, and localizing cetacean signals, and data can be processed and viewed in real-time (Jarvis *et al.*, 2014; Martin and Matsuyama, 2015; Moretti *et al.*, 2016). Fin whale calls were detected using the M3R low-frequency fast Fourier transform (FFT) detector, which creates binary detection spectrograms from time-frequency bins that cross an adaptive threshold (Jarvis *et al.*, 2014) and then classifies these detections by filtering by species specific temporal and spectral features (e.g., Martin and Matsuyama, 2015). Data were initially recorded in a proprietary packet format and later converted to FLAC using the MATLAB-based Raven-X toolbox (Dugan *et al.*, 2016; Dugan *et al.*, 2018). These files were downsampled to 1 kHz for fin whale analysis. The 8 TB hard drives utilized for acoustic recording on the SCORE array wrote data at an insufficient speed, which caused write errors as the data drives approached capacity (after  $\sim 96$  h of recording on each). This caused two major data dropouts as the first and then second disks filled,

resulting in loss of approximately 100 h of data per hydrophone (of 372 total deployment hours). A subset of 90 h of recordings (from 22 December 2015 05:00 UTC to 26 December 2015 02:00 UTC; the first continuous recording period before data write issues began) is used in the detection function and density estimation analysis.

### B. Fin whale tracking

Fin whale pulses were localized in two dimensions (latitude and longitude, without depth information) using TDOA methods similar to those described by Martin *et al.* (2015) for minke whales (*Balaenoptera acutorostrata*) and Helble *et al.* (2015) for humpback whales (*Megaptera novaeangliae*) at the U.S. Navy’s Pacific Missile Range Facility (PMRF). The method has previously been demonstrated to work for fin whales at SCORE (Ierley and Helble, 2016). Localizations were then grouped into “tracks” using a custom MATLAB (Mathworks, Natick, MA) routine (Martin and Matsuyama, 2015). The fin whale localization and tracking method is summarized in Fig. 2. Subsequent localizations were not connected or interpolated in any way, so the term “track” in this case means a set of localizations grouped temporally and spatially according to the settings outlined below. The tracking routine filters by the localization least squares estimate and the number of hydrophones that contributed to the localization, which helps remove spurious localizations. We allowed a maximum least squares value of 0.055 s and required detections from at least six hydrophones per localization. Localizations were grouped into tracks by setting a maximum distance threshold based on

known animal travel speeds and a maximum time threshold based on lengths of pauses between bouts of pulses. The maximum distance was set to 0.01° latitude and longitude, or approximately 1.1 km north to south and 0.9 km east to west at 32° N, and maximum time was set to 900 s between consecutive localizations. A minimum of eight localizations was required to constitute a track to exclude spurious localizations. The final settings balanced using only high-quality localizations and biologically realistic travel speeds while still providing a sufficient number of tracks for analysis.

### C. Detection function estimation

A snapshot detection function for the glider was modeled using a trial-based approach, with each trial consisting of a 360-s snapshot during which at least one fin whale track, meeting the above filtering criteria, was localized by the SCORE hydrophone array, and the glider was recording. Each trial, therefore, consisted of two 360-s data inputs: a track segment and a glider snapshot. To assess the feasibility of a trial-based approach to estimate detection probability, just the first 90 h of glider data were analyzed using the following detection probability estimation process (see Fig. 2 for overview of the process). A snapshot duration of 360 s was chosen to minimize potential whale movement while improving the ability to match pulse sequences across instruments. Based on mean fin whale travel speeds of 4–7 km h<sup>-1</sup> observed when fin whales were producing regular pulse sequences (Guazzo *et al.*, 2021; Hendricks *et al.*, 2021; Soule and Wilcock, 2013), we did not expect whales to travel more than 400–700 m per snapshot. This distance is

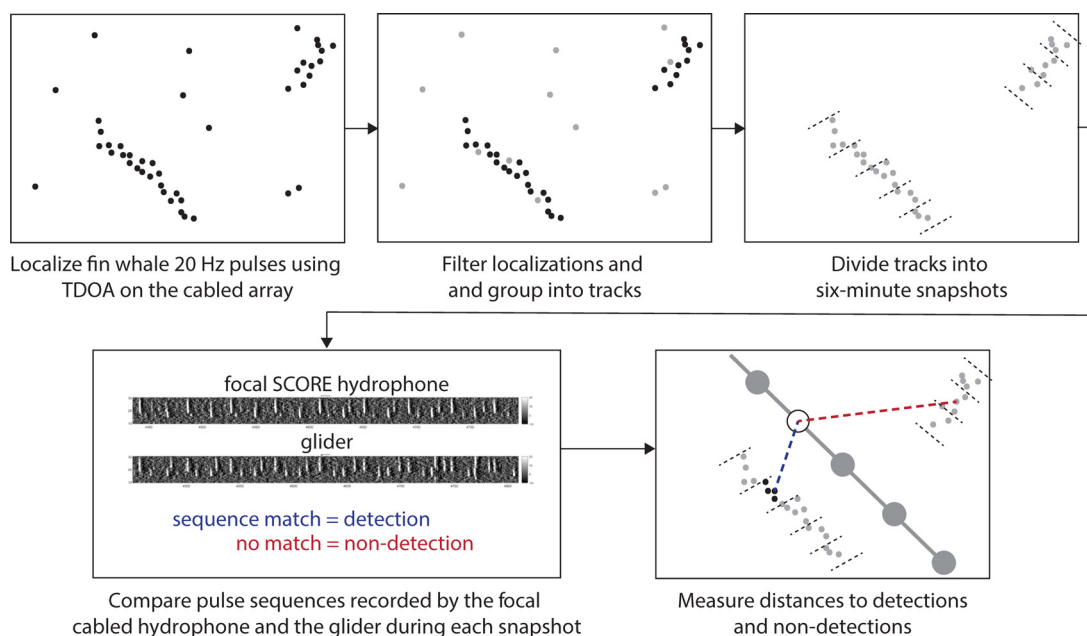


FIG. 2. (Color online) Flow chart outlining the steps from fin whale localizations to detection trials. Fin whale 20-Hz pulses are first localized using TDOA methods applied to the cabled array recordings. Localizations are filtered by accuracy and grouped into tracks. Tracks are then divided into 360-s snapshots. The spectrogram of the snapshot period recorded on the focal hydrophone (hydrophone with most localizations contributed to the track) was then cross-correlated with the spectrogram of the same time period recorded on the glider. If the sequence of pulses matched, the trial was scored as a detection (blue dashed line), and if no pulses were present on the glider recording or the sequence did not match, it was scored as a non-detection (red dashed line).

relatively small compared to known fin whale pulse detection ranges of tens of kilometers (Širović *et al.*, 2007; Stafford *et al.*, 2007). Conversely, 360 s is sufficient to capture natural variation in the generally stereotyped fin whale 20-Hz pulse, such as the brief rests in pulse sequences or deviation from the doublet pattern typically observed in these data. This natural variation was needed to match track segments to glider acoustic snapshots. Interpulse intervals typically ranged between 15 and 25 s, so each track segment and glider snapshot contained more than 20 pulses. The number of segments per track was dependent on the track length, averaging three segments (three glider snapshots) per track but having as many as 58 segments for the longest track.

We could not automatically assume that pulses recorded on the glider were the same pulses localized and tracked with the SCORE hydrophones, in other words, that all track segments paired with detections on the glider. Therefore, spectrograms of the glider snapshots and SCORE hydrophone recordings for track segment (each potential trial) were cross-correlated and visually inspected for inclusion in the final trial dataset and for assessment as a detection or non-detection on the glider.

For each track segment, a “focal hydrophone” was selected as the SCORE hydrophone that generated the most localizations in that track. If more than one hydrophone had the maximum number of localizations, the hydrophone closest to the track was set as the focal hydrophone. For each potential trial, spectrograms (2048 sample Hamming window, 90% overlap, frequency resolution 0.4883 Hz, time resolution 0.205 s) were generated for both the focal SCORE hydrophone data and the glider data from 1-kHz downsampled data. Spectrograms were trimmed to 10–30 Hz. Each spectrogram was equalized to remove continuous noise sources (e.g., vessels or flow noise) by subtracting the median levels of the preceding 4 s at each frequency.

Each glider snapshot spectrogram was cross-correlated to the focal SCORE hydrophone spectrogram for the corresponding track segment using normalized 2D cross correlation in MATLAB. The 2D spectrogram cross correlation allows for cross correlation of images in the time-frequency domain rather than time-amplitude domain waveforms; visual inspection of 2D spectrograms to confirm matches is more informative than one-dimensional waveforms for the human eyes. The SCORE spectrogram was padded with 66 s of data at the start and end to allow for differences in travel time of pulses traveling up to  $\sim 100$  km to each hydrophone (assumed sound speed  $1500 \text{ m s}^{-1}$ ). The cross correlation score and timing offset for the cross correlation peak were recorded for each snapshot, and spectrograms for the focal SCORE hydrophone and glider were plotted using the cross correlation offset to align them in time. Each trial was manually given a binary score as a detection or non-detection on the glider. If no pulses were visible on the glider spectrogram, the trial was marked as a “non-detection.” If the pattern of pulses on the glider and track segment focal

hydrophone matched, the trial was scored as a “detection.” If visual inspection of spectrogram plots, cross correlation scores, and cross correlation offset timing were unclear because of the presence of multiple whales or excessive glider noise, a potential trial was marked as “not sure” and was removed from further analysis. See supplementary Figs. 2 and 3<sup>1</sup> for example displays used for scoring. When multiple tracks overlapped in time, indicating the presence of multiple whales, multiple trial pairs of a given glider snapshot and various track segments were generated. Matching of sequences across the stationary and glider-generated spectrograms was often too difficult when multiple whales were present, so these overlapping potential trials were excluded from the detection function estimation to avoid potential ambiguity.

For each trial, horizontal distance from the mean of the track segment localizations within that 360-s glider snapshot to the mean dead-reckoned glider location [from the glide-slope model; Seaglider Quality Control Manual (University of Washington, 2016)] during the snapshot was estimated as the great-circle distance between two sets of latitude and longitude coordinates. Animal and glider depth were not accounted for in the horizontal distance estimation; distances were measured as if the track and glider were at the same depth. If no localizations were available within a given snapshot (the gap between subsequent track localizations could be as large as 900 s as set in the filtering process), no distance could be calculated, and that trial was removed. From previous work, we knew that 40-Hz spectral levels in the glider data were highly variable as a result of low-frequency flow noise (Fregosi *et al.*, 2020b); therefore, 40-Hz PSD levels were extracted for each glider snapshot and were included in the detection function model. The median 40 Hz noise level for each 360-s glider snapshot was calculated from the 1-min levels calculated above.

The detection probability for each trial as a function of range and 40-Hz spectral level was estimated using a generalized additive model (GAM; Wood, 2017). A GAM approach was chosen because it is more flexible than a generalized linear model—it does not require a detection function shape to be specified, allows the probability of detection at zero distance to be estimated, and does not require that the detection probability decreases monotonically with range. The response variable was the binary detection and non-detection score and was modeled as a Bernoulli trial with a logit link function. The explanatory variables were univariate thin plate regression splines for horizontal distance and median 40-Hz spectral level. A random effect for track number was included in the model because multiple trials from the same track cannot be considered independent samples. The model was fit using the *gam4* package (Wood and Scheipl, 2017) in program R (version 3.6.2; R Core Team, 2019).

The average snapshot detection probability is typically estimated by integrating the detection function from zero distance to some maximum distance, the truncation distance. An assumption of density estimates using trial-based

detection function methods is that the source (in this case, a fin whale) of an acoustic event detected on the glider is located within the specified truncation distance (Kyhn *et al.*, 2012; Marques *et al.*, 2009). If, in practice, the detection probability is not zero by this truncation distance, then the assumption that all detected events occurred within the truncation distance does not hold. Detected animals may be located beyond this truncation distance, resulting in an underestimate of the effective survey area and an overestimate of density. For the trials with the lowest median noise levels on the glider (<89 dB), animals were detected out to the maximum horizontal distance available in this study (50 km; supplementary Fig. 5),<sup>1</sup> resulting in the probability of detection for all trials not reaching zero as required by the trial-based approach. To address this, a detection function was calculated for just trials with 40-Hz spectral levels between 90 and 100 dB (dB levels rounded to the nearest integer value). A lower bound of 90 dB was used because there was a mix of detections and non-detections at this noise level at the maximum distance of 50 km (supplementary Fig. 5).<sup>1</sup> A single median detection function was calculated for this subset of data based on the median noise level for trials with glider noise levels from 90 to 100 dB.

Effective survey area,  $\hat{a}_e$ , was calculated from the estimated noise band limited detection function following point-transect distance sampling methods (Buckland *et al.*, 2001) and the equation

$$\hat{a}_e = 2\pi \int_{r=0}^w yg(y)dy, \tag{1}$$

where  $g(y)$  is the detection function, which estimates the probability of detection at horizontal range  $y$ , and  $w$  is the truncation distance, defined in this case as the range at which probability of detection is essentially zero. A value of 60 km was used for  $w$  because of the size and localization limits of the SCORE array and the need to exclude low noise level trials to limit maximum detection ranges within SCORE. Effective detection radius (EDR) was calculated using

$$EDR = \sqrt{\frac{\hat{a}_e}{\pi}}. \tag{2}$$

Because variance estimates for non-independent data can be underestimated, variances for  $\hat{a}_e$  and EDR calculations were estimated empirically using a jackknife procedure with glider dive number as the resampling unit (Efron, 1982). The coefficient of variation (CV) is presented as the measure of precision and was calculated as the standard error divided by the mean.

## D. Density estimation

### 1. Glider

The density of acoustic events and of individual animals was estimated from the glider-collected acoustic data using

a point-transect approach (Buckland *et al.*, 2001), where the glider path was divided into snapshots, each representing a sampling point. An acoustic event as recorded on the glider was defined as a 360-s snapshot with 40-Hz spectral levels between 90 and 100 dB containing fin whale 20-Hz pulses. Acoustic events were scored manually by visual inspection of spectrograms of each possible 360-s snapshot. The density of acoustic events,  $\hat{D}_s$ , was estimated as

$$\hat{D}_s = \frac{n}{k\hat{a}_e}, \tag{3}$$

where  $n$  is the number of acoustic events detected,  $k$  is the total number of 360-s snapshots with 40-Hz spectral levels between 90 and 100 dB recorded by the glider, and  $\hat{a}_e$  is the effective survey area estimated with Eq. (1). Variance for the proportion of snapshots with pulses ( $n/k$ ) was estimated empirically using a jackknife approach with glider dive ( $n=16$ ) as the resampling unit (Efron, 1982). No estimate of false-positive rate, as is typically included in acoustic density estimation based on automated detections, is needed because all detections were marked manually, and uncertain detections were not included.

The density of individual fin whales,  $\hat{D}$ , was then estimated by accounting for the probability of a fin whale producing pulses in a 360-s snapshot and the number of fin whales producing pulses in any given snapshot using

$$\hat{D} = \frac{n\hat{s}}{k\hat{a}_e\hat{P}_p} \tag{4}$$

or

$$\hat{D} = \frac{\hat{D}_s\hat{s}}{\hat{P}_p}, \tag{5}$$

where  $\hat{P}_p$  is the estimated probability that a fin whale will be available for detection, meaning a fin whale is producing pulses within a 360-s snapshot (hereafter called acoustic availability), and  $\hat{s}$  is the estimated number of fin whales producing pulses (acoustically active group size) in any given snapshot. The acoustic availability,  $\hat{P}_p$ , was estimated from acoustic behavior data of ten tagged fin whales in Southern California, where tag accelerometer data allowed for pulses to be attributed to the tagged animal with certainty (Goldbogen *et al.*, 2014; Stimpert *et al.*, 2015), and was estimated in two ways—weighted by tag duration and weighted equally across all tags. For a vocalization type like fin whale song that is known to be made only by males during the breeding season and is highly repetitive for hours at a time, it may be more appropriate to not weight vocal behavior by tag duration; with a small set of whales sampled ( $n=10$  tag deployments), this could minimize the effect of highly variable tag durations on different whales. Because of this uncertainty, we estimated density using both



approaches. Each tag record was divided into 360-s snapshots, and the proportion of snapshots containing pulses produced by the tagged animal was calculated. The proportion of snapshots with pulses was calculated for each tagged animal as the mean of the proportions for all possible snapshot start times (0–359 s into the tag record) to correct for any potential bias due to an arbitrary choice of where the snapshot starts in the tag acoustic record. Mean acoustic availability was then calculated as the sum of all proportions of snapshots with pulses divided by the number of tags (unweighted) or as the sum of all proportions of snapshots with pulses, weighted by tag duration, and divided by the total duration of all tags (weighted). Variance for the unweighted acoustic availability was calculated using a jackknife approach with tag number as the resampling unit. Variance in the weighted acoustic availability was estimated from the between-tag variation in proportion of snapshots containing pulses, weighted by tag deployment length [see Ward *et al.* (2012), Eqs. (5) and (6)]. Stimpert *et al.* (2015) did not find any relationship between group size and acoustic behavior. However, when quantifying the proportion of snapshots containing fin whale pulses ( $n/k$ ), there was evidence that some snapshots may have contained pulses from multiple individuals (as evidenced by pulse sequences with different received levels and timing patterns). If it is assumed each snapshot only contained pulses from a single acoustically active whale, the density estimate may be biased low. To account for this, the average number of acoustically active whales in a given snapshot ( $\hat{s}$ ) was estimated from the tracking data as the mean number of tracks across all snapshots with noise levels from 90 to 100 dB that contained at least one track. Variance for  $\hat{s}$  was also estimated using a jackknife approach with glider dive number as the resampling unit.

Variance in the density estimate was calculated from the combined CV values of the proportion of snapshots with pulses, effective survey area, acoustically active group size, and acoustic availability parameters using an approximation of the delta method (Marques *et al.*, 2013; Seber, 1982). Confidence intervals (CI; 95%) were estimated by assuming a lognormal distribution of estimated density, following Buckland *et al.* (2015).

## 2. SCORE

For comparison, density was estimated for the same area and time period using a plot sampling approach similar to Moretti *et al.* (2010) and Ward *et al.* (2012). Assuming that all pulse-producing fin whales within the SCORE array can be tracked and counted, the number of fin whale tracks within the array boundary during a 360-s snapshot was used as the acoustic events of interest. Density,  $\hat{D}$ , was estimated as

$$\hat{D} = \frac{n_t}{kA\hat{P}_p}, \quad (6)$$

where  $n_t$  is the number of tracked whales counted over  $k$  360-s snapshots,  $A$  is the total area of the array, calculated as the convex hull of the array, and  $\hat{P}_p$  is the same probability of a fin whale producing pulses in a 360-s snapshot, estimated from tag data (Stimpert *et al.*, 2015) and used in Eq. (4).

Variance of the number of tracked whales per snapshot,  $n_t/k$ , was estimated empirically using a jackknife approach because subsequent snapshots cannot be considered independent. Six-hour blocks were used as the jackknife resampling unit as that was the approximate glider dive length used in the variance calculations for Eq. (4). Variance in the density estimate was calculated from the combined CV values of the number of whales per snapshot and the acoustic availability using an approximation of the delta method (Marques *et al.*, 2013; Seber, 1982), and 95% confidence intervals were estimated assuming a lognormal distribution of estimated density.

## III. RESULTS

### A. Trial-based detection function

A total of 77 tracks occurred during the 90 h of analyzed glider recordings and were located throughout the study area (Fig. 3). These tracks generated 859 trials of 360 s duration that were manually scored (415 detections, 174 non-detections, 270 excluded for non-definitive assessment; supplementary Figs. 4 and 5).<sup>1</sup> Spectral levels at 40 Hz varied with glider dive cycles in a predictable pattern, with higher levels during the glider descent and lower levels during ascents (Fig. 4). All noise levels reported are PSD levels in dB re 1  $\mu\text{Pa}^2/\text{Hz}$ . Levels at 40 Hz were generally between 80 and 105 dB. The decrease in 40-Hz levels from the start to the end of a dive cycle is due to faster glider speed during descents and slower glider speed during ascents. Glider pumping activity, which lasts several minutes at the bottom of each dive cycle, is the source of the levels near 120 dB.

The final subset of trials with glider noise levels between 90 and 100 dB that was used to model the detection function included 165 trials from 37 tracks and consisted of 80 detections and 85 non-detections (Fig. 5). Differences in detectability at increased horizontal distances and higher noise levels occurred generally as expected from simple spherical spreading acoustic transmission loss and masking, with fewer detections at greater horizontal distances and higher noise levels (Fig. 5). At the quieter noise levels ( $\sim 90$  dB), the detection function shows a shoulder with detections certain up to about 30 km and then a monotonic drop as horizontal distance increases (Fig. 6). Detection probability at horizontal distance zero is certain when 40 Hz noise levels were between 90 and 96 dB but drops to 0.7 at 100 dB noise level. The median noise level for all trials with 40-Hz levels between 90 and 100 dB was 97 dB, and at that noise level, the modeled maximum detection range is almost 40 km (Fig. 6). Effective survey area,  $\hat{a}_e$ , for the median detection probability at noise levels of 97 dB was estimated

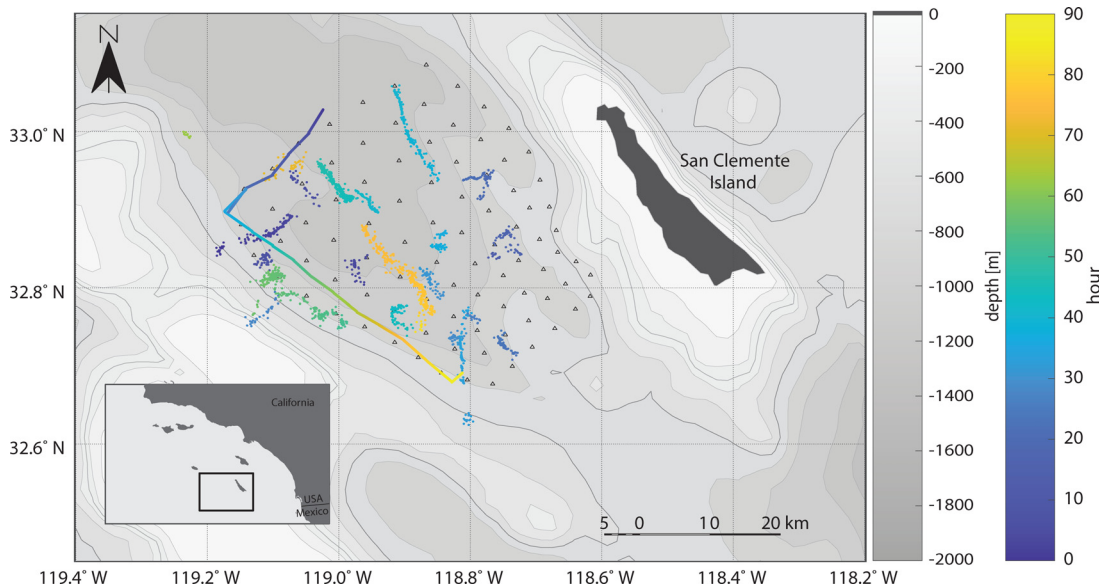


FIG. 3. (Color online) Fin whale localizations and the glider track. Localizations that make up whale tracks are shown as colored points; color represents time in hours from the start of the glider deployment. The glider track is shown as the colored line with the same colormap as the localizations and is generated from straight-line interpolation between surface GPS positions. Black triangles show approximate location of the SCORE hydrophone array; for security reasons, exact locations cannot be shown. Bathymetry data are from NOAA's National Centers for Environmental Information (Amante and Eakins, 2009).

to be  $915.9 \text{ km}^2$  [jackknife CV ( $CV_j$ ) = 0.26]; EDR was  $17.1 \text{ km}$  ( $CV_j = 0.13$ ).

**B. Estimated density**

The 90-h survey spanned 18 glider dives (dives 7–24), and 343 snapshots recorded by the glider had 40-Hz spectral levels between 90 and 100 dB [mean 19.1 snapshots per dive; standard deviation (SD) 5.43; supplementary Table I].<sup>1</sup> The proportion of snapshots with fin whale 20-Hz pulses,  $n/k$ , was 0.47 ( $CV_j = 0.12$ ), and the density of pulse-present snapshots was 0.53 pulse-present snapshots per  $1000 \text{ km}^2$  ( $CV_j = 0.23$ ; 95% CI 0.34–0.83). The average number of

acoustically active whales tracked within a single snapshot (with at least one whale present;  $\hat{s}$ ) was 1.3 whales ( $CV_j = 0.071$ ). Acoustic availability, or the probability of a fin whale vocalizing in a 360-s snapshot,  $\hat{P}_p$ , as calculated from tagging data presented in Stimpert et al. (2015), was 0.35 ( $CV = 0.46$ ) when weighted by tag duration and 0.26 ( $CV_j = 0.48$ ) if not weighted by tag duration. Fin whale density, using the weighted acoustic availability, as estimated from the glider 90-h survey, was 1.8 whales per  $1000 \text{ km}^2$  ( $CV = 0.55$ ; 95% CI 0.67–5.0; Table I). Using the unweighted acoustic availability, the estimate was 2.5 whales per  $1000 \text{ km}^2$  ( $CV = 0.56$ ; 95% CI 0.88–6.89; Table I).

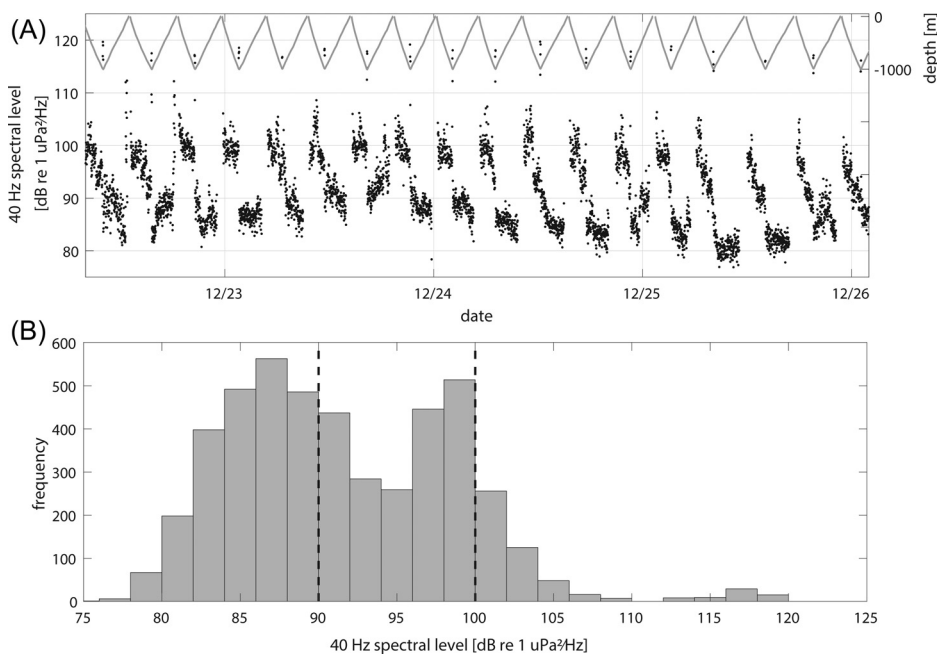


FIG. 4. (A) 40-Hz spectral levels recorded on the glider in 1-min intervals (black dots) and glider dive profile (gray line, right y axis) and (B) histogram distribution of noise levels for the first 3 days of the survey. Vertical dashed lines in the histogram indicate the 90 and 100 dB limits that were used to select the final trials included in the detection function and density estimate.

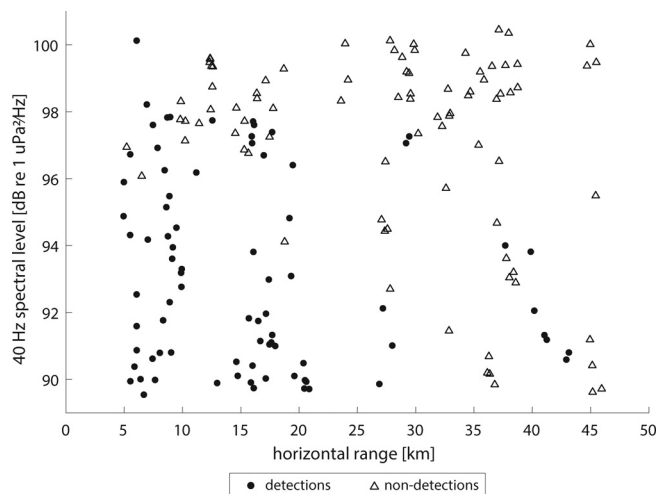


FIG. 5. Snapshots that were detected (black circles) or not detected (out-lined black triangles) by the glider as a function of distance from the track segment to the glider and the median 40-Hz spectral level for the corresponding snapshot. Only the subset of snapshots ( $n=165$ ) used in the detection function analysis are displayed. An analogous figure displaying all possible snapshots is available as supplementary Fig. 5 (see Footnote 1).

The total area of the SCORE array is  $1381.2 \text{ km}^2$ , and there were, on average, 0.63 tracked, acoustically active whales per 360-s snapshot (900 total snapshots,  $\text{CV}_j = 0.16$ ). Fin whale density, as estimated from the SCORE hydrophones during the same period, was 1.3 and 1.7 whales per  $1000 \text{ km}^2$ , using the weighted and unweighted acoustic availability, respectively (weighted:  $\text{CV} = 0.49$ ; 95% CI 0.52–3.2; unweighted:  $\text{CV} = 0.51$ ; 95% CI 0.67–4.4; Table I).

IV. DISCUSSION

We demonstrate that (1) a detection function for an acoustic glider can be estimated using a trial-based method, using whale tracks localized by a cabled array and the simultaneous glider recordings as the trials and that (2)

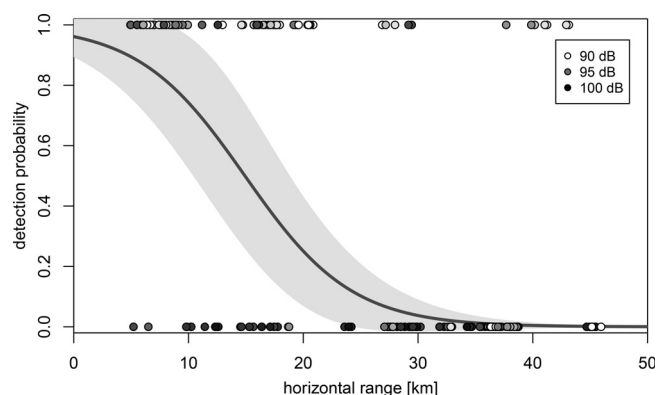


FIG. 6. Median snapshot detection probability estimated from snapshots with 40 Hz spectral levels between 90 and 100 dB re  $1 \mu\text{Pa}^2/\text{Hz}$  at the median noise level of 97 dB re  $1 \mu\text{Pa}^2/\text{Hz}$ . Detection probability was dependent on distance and 40 Hz noise level. Gray shading indicates the 95% confidence interval, and raw binary trial scores are plotted as circles, shaded by the 40 Hz spectral level for each trial.

TABLE I. Density estimates (per  $1000 \text{ km}^2$ ), jackknife ( $\text{CV}_j$ ), and 95% confidence of density estimates for fin whales from the glider and SCORE acoustic data. Densities are estimated using both a weighted acoustic availability, which weights pulse-present snapshot rates by tag deployment durations, and unweighted acoustic availability, where tags are weighted equally when estimating the pulse-present snapshot rate.

Data source	Weighted acoustic availability			Unweighted acoustic availability		
	Density ( $\hat{D}$ )	CV	95% CI	Density ( $\hat{D}$ )	CV	95% CI
Glider	1.8	0.55	0.67–5.0	2.5	0.56	0.88–6.9
SCORE	1.3	0.49	0.52–3.2	1.7	0.51	0.67–4.4

density can be estimated from glider-collected acoustic data using an approach based on point-transect distance sampling. Results indicate that glider flow noise, in the adjacent frequency band as the fin whale pulses of interest, is an important covariate in the detection function, and therefore noise levels are a critical consideration in estimating fin whale density. The glider-based and SCORE estimates of density are similar, but both have large variance, primarily due to limited data on fin whale acoustic behavior.

A. Detection function estimates

The estimated EDR and maximum detection range for the glider were similar to previous estimates for fin whale detection ranges and effective survey areas (Harris *et al.*, 2018; Širović *et al.*, 2007; Širović *et al.*, 2015; Stafford *et al.*, 2007). The detection probability for the glider was higher than that estimated using a propagation modeling approach (Stafford *et al.*, 2007). Stafford *et al.* (2007) found a steep drop-off in detection probability with near-zero probability at only 10 km when ambient noise levels at 25 Hz were 91 dB. The differences in detection probability could be because of different bathymetry, instrumentation, or different units of detection (single pulses vs pulse presence within a snapshot) mediated by the season of the glider survey. The glider work took place in the winter when male fin whales are typically producing long bouts of pulses as song, which meant that there is a greater probability that multiple pulses are detected and so pulse presence in a snapshot is more detectable than short intermittent series of 20-Hz pulses that are more common in the summer (Thompson and Friedl, 1982; Watkins *et al.*, 2000).

A primary limitation of this work is that the collected data did not include trials with horizontal ranges between the glider and tracked whales that were greater than 50 km. When counting snapshots with acoustic events present, it is necessary to know with certainty that any pulses in a detected snapshot were produced within a defined maximum detection radius, i.e., the truncation distance. If the detection function does not reach zero at this truncation distance, it is not given that the pulses detected within any snapshot were produced within that maximum distance; pulses may be detected that originated beyond the maximum distance, which would bias density estimates high. For a target species such as a fin whale, it would have been preferable to



have maximum trial distances up to 100 km (Stafford *et al.*, 2007). In quiet conditions, we might expect fin whales to be heard that far (Stafford *et al.*, 2007) and so would ideally estimate the detection function out to that range. In this work, the variability in noise levels in the frequencies of and near fin whale 20-Hz pulses on the glider allowed for a reasonable detection probability to be estimated using the limited available trial distances. The low-frequency flow noise varied predictably with the glider's speed as a result of the glider's ballasting and flight parameters. Descents were significantly faster, and flow noise was higher than during ascents (Fregosi *et al.*, 2020b). Analyzing a subset of trials with intermediate 40 Hz spectral levels (between 90 and 100 dB) ensured the detection function tail dropped to zero at the maximum ranges. Future efforts could direct the glider to survey off SCORE with the idea that whales at large distances from the glider but within SCORE could be localized, and increased distances could be included in the trial. The bathymetry at SCORE may limit such an approach; San Clemente Island borders the range to the east, and west of the hydrophone array is relatively shallow water. Operating the glider north of the hydrophone array may provide the best opportunity to improve the available distances, though it is important to design the trial so that the resulting detection function is representative of the study area in general, i.e., that there is no spatial or temporal bias introduced when conducting the trial in a geographic area different from the primary area of interest.

Additional biases in this detection function could be due to the localization, tracking, and filtering processes used to generate the detection trials, but we believe these do not detract from the demonstration of estimating a detection function for a glider. The localization and tracking process implemented here is regularly used for studies of baleen whale behavior on U.S. Navy ranges (Helble *et al.*, 2015; Martin *et al.*, 2015). Foremost, it is important to state the glider detection function is for trackable whales, meaning only those whales that exhibited acoustic behavior and were present in a location that the existing SCORE detection, classification, and localization process was able to identify. We assume that there is no difference in detectability for trackable and non-trackable whales in our estimate of total fin whale density, but we do not have empirical evidence for this in this study. An individual producing pulses in regular sequences is likely more trackable than an individual producing intermittent pulses because of specified tracking and filtering parameters used (minimum number of hydrophones, minimum number of localizations required to constitute a track). We addressed this by also using sequences of pulses (within a 360-s snapshot) as the detected acoustic event. However, being able to restrict detections by this criterion was only possible because of the abundance of pulse sequences available during this winter survey. A comparison with fin whale trackability in summer months may provide insight into the appropriateness of this assumption and how it may best be accounted for. The number of available tracks and whales available in this relatively short experiment

allows the filtering to be relatively restrictive, including only high-quality localizations (least squares score- $<0.055$  s) and those with more than the minimum number of necessary hydrophones (six versus four). Further, track locations were not interpolated; if there was a gap in track localizations over a particular snapshot, that snapshot was not used as a trial. This meant no assumptions of animal location between localizations were needed, although by our estimates this would likely not have been an issue (based on average travel distances of a few hundred meters in 6 min compared to detection ranges over 10 km). Tracks with more relaxed filtering or using interpolated locations need to be explored to better understand these potential biases.

This detection function is specific to Southern California (specifically the SCORE area) during the fall and winter when male fin whales are singing. Application of the detection function presented here to longer-duration glider surveys or surveys where it is not possible to estimate a survey-specific detection function (because no auxiliary information about animal locations is available) may be appropriate for estimating fin whale density if the same noise level restriction is applied to the snapshot detection process of the external survey. Noise at 40 Hz was a key parameter in the detection function, and accounting for noise levels may allow this detection function to be carefully applied to additional surveys. In general, however, the aim should be to obtain survey-specific detection functions wherever possible (Marques *et al.*, 2013). More work on variability in detection functions across regions and seasons is needed to understand the potential variability in detection functions for gliders. Low-frequency, glider-generated flow noise is a dominant component of glider recordings (Fregosi *et al.*, 2020b; Matsumoto *et al.*, 2015; dos Santos *et al.*, 2016), and measuring this noise is relatively straightforward. The effect of ambient noise on detectability (Helble *et al.*, 2013; Ward *et al.*, 2011) is negligible compared to the effect of glider-generated flow noise (Fregosi *et al.*, 2020b). While restricting snapshots by the 40-Hz noise level could introduce bias by removing a specific subset of data points, we can assume the total number of whales does not change with flow noise levels on the glider because the noise on the glider is tied directly to glider speed rather than environmental conditions (e.g., weather, sound propagation, presence of ships). Thus, in this case, removing data points based on glider noise levels is not introducing bias in our animal density estimate.

The manual matching and detection process used in this work was labor intensive and, while important for this initial demonstration, may be difficult to implement for a longer-duration study. However, it would be possible to extend the method to account for potential mis-associations (Caillat *et al.*, 2013). A fully automated cross correlation process to match tracked fin whales to fin whales detected on the glider was not possible, primarily because there was such an abundance of fin whale pulses, with many instances of multiple animals detectable and some very distant pulses and multi-path detections. Because the more “difficult-to-score” trials,



where multiple animals were present or pulses were very faint, were excluded, there may be bias in the density estimate. A more streamlined and unambiguous process for a detection versus a non-detection that required a minimum or maximum number of pulses or a minimum signal-to-noise ratio would be beneficial in the future.

Including glider depth as a covariate in the detection function was not possible in this study because glider depth and 40-Hz noise level were correlated (increasing noise level at shallower depths), so they could not both be included in the GAM. However, this observed correlation was driven by the snapshots with mean glider depths from 200 to 400 m; these snapshots had only relatively high noise levels (>96 dB). If only snapshots with glider depths of 400 m or greater were examined, there was no correlation between glider depth and 40-Hz noise level, and including depth as a covariate in the GAM did not improve the model. Although sound propagation can vary with depth, previous work (using the glider-collected acoustic data from this same experiment) showed that the number of detections of individual fin whale 20-Hz pulses did not vary with glider depth (Fregosi *et al.*, 2020b). It is possible the high variability of 40-Hz noise levels dominates the detection function results and limited our ability to investigate the possibly minor role of depth. Depth as a covariate in detection functions warrants more research and may be able to be investigated in an experiment without the strong influence of 40 Hz flow noise.

## B. Estimated density

The overlap of the glider survey with the SCORE array not only allowed us to estimate a detection function for a single-hydrophone system; it also gave us the unique opportunity to compare two acoustic density estimate methods for the same time and place. The density of fin whales estimated from the acoustic glider (1.8 whales per 1000 km<sup>2</sup>) is higher compared to the SCORE estimate (1.3 whales per 1000 km<sup>2</sup>), but because of the large variance in both estimates, their 95% confidence intervals overlap considerably (Table I). The estimates are for the same time period and same general location but do not cover the exact same area, so some difference is not unexpected. The actual distribution of the tracked whales (Fig. 3) supports a somewhat higher density estimate by the glider because more of the tracked whales occurred on the western portion of the range or off the range to the west, within the glider's effective survey area.

Both the glider and SCORE estimates are similar to the overall density of fin whales in Southern California from 2004 to 2013 estimated from a visual line-transect survey (2.7 whales per 1000 km<sup>2</sup>) by Campbell *et al.* (2015). The CVs of the glider-generated and SCORE estimates are more than double that of Campbell *et al.* (2015) (CV = 0.19), likely because of the high variance of the acoustic availability parameter, which was calculated from only a small sample of tagged fin whales. However, comparing just the winter season, the glider estimate is almost four times larger

than that from the visual surveys (0.65 whales per 1000 km<sup>2</sup>), where peak densities occurred in summer and fall (Campbell *et al.*, 2015). Variance on the visual estimate for winter is higher than the overall estimate and is closer to the variance of the glider-generated estimate (0.42; Campbell *et al.*, 2015). While it is useful to generally compare the glider-generated density estimate to that of historical visual line-transect surveys, the glider survey covered a much smaller area and time compared to Campbell *et al.* (2015). For this reason, we do not suggest using these particular glider-based or SCORE estimates to make conclusions about changes in population trends, as was possible in Campbell *et al.* (2015).

Parameters in the density estimator necessary to convert acoustic event density to animal density should ideally be collected from the survey region and time period where the survey takes place. Density estimation assumes these parameters are accurate for the time and place of the main survey. The estimate of acoustically active group size was taken from the exact area and time of the survey, but it assumes that all acoustically active animals were tracked and that only a single animal made up each track, which may not always be a valid assumption. If all acoustically active animals are not tracked, or if a single localized track was actually based on pulses generated by multiple animals, then the acoustically active group size estimate, and therefore density, is likely underestimated.

The tagged animal estimate of acoustic availability applied here is for fin whales in Southern California and is the best available acoustic behavior data we have for fin whales, but it comes from a low sample size of tagged whales and is likely to be inaccurate for the acoustic availability parameter required here. Stimpert *et al.* (2015) aimed to quantify behavior of fin whales that were and were not producing pulses and, therefore, did not differentiate between 20- and 40-Hz pulses (which were not used in this study), but they do state that most recorded pulses were the 20-Hz type. The tagging work occurred in the fall (September and October), and the glider survey occurred in December and January. In estimating total fin whale density, we assume the population structure (i.e., age, sex) of the tagged whales is representative of the population structure of all fin whales in this area in all seasons. This assumption may not hold if tagging efforts are biased toward one sex or age class or if population demographics vary across geographic areas or seasons. For example, if permitting did not allow tagging of females with calves, it is possible fewer females were tagged, which would mean the probability of a whale vocalizing would be biased high and the density estimate would be biased low. It was also unclear whether it was better to weight the data by tag duration or use per-whale weighting, i.e., to weight each tag deployment equally. While a previous study estimating density of sperm whales did weight the tags by tag duration (Ward *et al.*, 2012), that target sound was echolocation clicks that are made by all individuals regardless of age or sex class. To deal with this uncertainty, we presented both approaches

here and show that the large variance in the resulting density overshadows any potential difference in weighting approach.

By comparing the CV of the acoustic event density (0.2) and the CV of fin whale density (0.55), it is clear that adjustment for acoustic availability has the greatest effect on the variance of the density estimate. Because of the small size of the tag dataset and the large confidence intervals on the density estimate (0.9–7.1 animals per 1000 km<sup>2</sup>), the density estimate provided here is presented as an example of how animal density could be estimated if appropriate distance-estimation parameters are available but should not be widely extrapolated to the larger Southern California Bight region or used to infer changes in population size. Because we estimated and present acoustic event density here, animal density can be updated in the future if more accurate acoustic availability data become available.

## V. CONCLUSIONS

The ability to use acoustically equipped gliders to estimate cetacean population density has the potential to greatly expand our capabilities for long-term and broad spatial monitoring of cetaceans. This work provides one possible framework for estimating cetacean density from an acoustic glider, an empirical detection function for fin whales recorded by a glider, and a proof-of-concept density estimate of fin whales for a small example 90-h survey. The approach used—leveraging the ability of an array to track individual animals and setting up detection trials with those tracks—could be applied in other regions and to other whale species that are also trackable through an array.

## ACKNOWLEDGMENTS

The authors thank Alex Turpin (Oregon State University) for his work on implementing the acoustic system on the glider and floats and for his help in the field, Ronald Morrissey (Naval Undersea Warfare Center) and the crew of the *RSC4* for assistance with the field work, and Anatoli Erofeev (Oregon State University) for glider piloting services and expertise. Special thanks to Tyler Helble and Len Thomas for discussions of fin whale tracking and density estimation and Janelle Badger for help with plotting model results. Funding for this work was provided by Living Marine Resources Program Grant No. N39430-14-C-1435 and Office of Naval Research Grant No. N00014-15-1-2142. S.F. was supported by the Department of Defense National Science and Engineering Graduate Fellowship. This is Pacific Marine Environmental Laboratory (PMEL) Contribution No. 5101.

<sup>1</sup>See supplementary material at <https://www.scitation.org/doi/suppl/10.1121/10.0014793> for additional tables and figures, including raw data on the number of snapshots containing fin whale pulses per glider dive, sound speed profile data collected by the glider, example figures of the cross correlation process, and exploratory plots of all potential trials at all noise levels.

- Amante, C., and Eakins, B. W. (2009). "ETOPO1 1 arc-minute global relief model: Procedures, data sources and analysis," NOAA Technical Memorandum NESDIS NGDC-24 (National Geophysical Data Center, Boulder, CO).
- Barlow, J., and Forney, K. A. (2007). "Abundance and population density of cetaceans in the California Current ecosystem," *Fish. Bull.* **105**, 509–526.
- Barlow, J., Fregosi, S., Thomas, L., Harris, D. V., and Griffiths, E. T. (2021). "Acoustic detection range and population density of Cuvier's beaked whales estimated from near-surface hydrophones," *J. Acoust. Soc. Am.* **149**, 111–125.
- Barlow, J., and Taylor, B. L. (2005). "Estimates of sperm whale abundance in the northeastern temperate Pacific from a combined acoustic and visual survey," *Mar. Mammal Sci.* **21**, 429–445.
- Barlow, J., Tyack, P. L., Johnson, M. P., Baird, R. W., Schorr, G. S., Andrews, R. D., and Aguilar de Soto, N. (2013). "Trackline and point detection probabilities for acoustic surveys of Cuvier's and Blainville's beaked whales," *J. Acoust. Soc. Am.* **134**, 2486–2496.
- Baumgartner, M. F., Fratantoni, D. M., Hurst, T. P., Brown, M. W., Cole, T. V. N., Van Parijs, S. M., and Johnson, M. P. (2013). "Real-time reporting of baleen whale passive acoustic detections from ocean gliders," *J. Acoust. Soc. Am.* **134**, 1814–1823.
- Buckland, S. T. (2006). "Point-transect surveys for songbirds: Robust methodologies," *Auk* **123**, 345–357.
- Buckland, S. T., Anderson, D. R., Burnham, K. P., Laake, J. L., Borchers, D. L., and Thomas, L. (2001). *Introduction to Distance Sampling* (Oxford University, Oxford, UK).
- Buckland, S. T., Rexstad, E. A., Marques, T. A., and Oedekoven, C. S. (2015). *Distance Sampling: Methods and Applications Methods in Statistical Ecology* (Springer, Cham, Switzerland).
- Caillat, M., Thomas, L., and Gillespie, D. (2013). "The effects of acoustic misclassification on cetacean species abundance estimation," *J. Acoust. Soc. Am.* **134**, 2469–2476.
- Campbell, G. S., Thomas, L., Whitaker, K., Douglas, A. B., Calambokidis, J., and Hildebrand, J. A. (2015). "Inter-annual and seasonal trends in cetacean distribution, density and abundance off southern California," *Deep. Res. Part II Top. Stud. Oceanogr.* **112**, 143–157.
- Carretta, J. V., Forney, K. A., Oleson, E. M., Weller, D. W., Lang, A. R., Baker, J., Muto, M. M., Hanson, B., Orr, A. J., Huber, B., Lowry, M. S., Barlow, J., Moore, J. E., Lynch, D., Carswell, L., and Brownell, R. L., Jr. (2020). "U.S. Pacific marine mammal stock assessments: 2019," NOAA Technical Memorandum NMFS-SWFSC-629, U.S. Department of Commerce, Washington, DC.
- Cauchy, P., Heywood, K. J., Risch, D., Merchant, N. D., Queste, B. Y., and Testor, P. (2020). "Sperm whale presence observed using passive acoustic monitoring from gliders of opportunity," *Endang. Species Res.* **42**, 133–149.
- Croll, D. A., Clark, C. W., Acevedo, A., Tershy, B., Flores, S., Gedamke, J., and Urban, J. (2002). "Only male fin whales sing loud songs," *Nature* **417**, 809.
- dos Santos, F. A., São Thiago, P. M., de Oliveira, A. L. S., Barmak, R., Lima, J. A. M., de Almeida, F. G., and Paula, T. P. (2016). "Investigating flow noise on underwater gliders acoustic data," *J. Acoust. Soc. Am.* **140**, 3409–3409.
- Dugan, P., Zollweg, J., Roch, M., Helble, T., Pitzrick, M., Clark, C., and Klinck, H. (2018). "The Raven-X software package: A scalable high-performance computing framework in Matlab for the analysis of large bioacoustic sound archives," [https://zenodo.org/record/1221417#\\_ZyOCpXbMK3B](https://zenodo.org/record/1221417#_ZyOCpXbMK3B) (Last viewed 10/12/2022).
- Dugan, P. J., Klinck, H., Roch, M. A., and Helble, T. A. (2016). "RAVEN-X: A high performance data mining toolbox for bioacoustic data analysis," ONR Report No. N00014-16-1-3156, Office of Naval Research, Arlington, VA.
- Efron, B. (1982). *The Jackknife, the Bootstrap and Other Resampling Plans* (Society for Industrial and Applied Mathematics, Philadelphia, PA).
- Fregosi, S., Harris, D. V., Matsumoto, H., Mellinger, D. K., Barlow, J., Baumann-Pickering, S., and Klinck, H. (2020a). "Detections of whale vocalizations by simultaneously deployed bottom-moored and deep-water mobile autonomous hydrophones," *Front. Mar. Sci.* **7**, 721.
- Fregosi, S., Harris, D. V., Matsumoto, H., Mellinger, D. K., Negretti, C., Moretti, D. J., Martin, S. W., Matsuyama, B., Dugan, P. J., and Klinck, H. (2020b). "Comparison of fin whale 20 Hz call detections by deep-water

- mobile autonomous and stationary recorders," *J. Acoust. Soc. Am.* **147**, 961–977.
- Gerrodette, T., Taylor, B. L., Swift, R., Rankin, S., Jaramillo-Legorreta, A. M., and Rojas-Bracho, L. (2011). "A combined visual and acoustic estimate of 2008 abundance, and change in abundance since 1997, for the vaquita, *Phocoena sinus*," *Mar. Mamm. Sci.* **27**, E79–E100.
- Gkikopoulou, K. C. (2018). "Getting below the surface: Density estimation methods for deep diving animals using slow autonomous underwater vehicles," Ph.D. thesis, University of St Andrews, St Andrews, Scotland.
- Glennie, R., Buckland, S. T., and Thomas, L. (2015). "The effect of animal movement on line transect estimates of abundance," *PLoS One* **10**, e0121333.
- Goldbogen, J. A., Stimpert, A. K., DeRuiter, S. L., Calambokidis, J., Friedlaender, A. S., Schorr, G. S., Moretti, D. J., Tyack, P. L., and Southall, B. L. (2014). "Using accelerometers to determine the calling behavior of tagged baleen whales," *J. Exp. Biol.* **217**, 2449–2455.
- Guazzo, R. A., Durback, I. N., Helble, T. A., Alongi, G. C., Martin, C. R., Martin, S. W., and Henderson, E. E. (2021). "Singing fin whale swimming behavior in the central north Pacific," *Front. Mar. Sci.* **8**, 696002.
- Harris, D. V., Fregosi, S., Klinck, H., Mellinger, D. K., Barlow, J., and Thomas, L. (2017). "Evaluating autonomous underwater vehicles as platforms for animal population density estimation," *J. Acoust. Soc. Am.* **141**, 3606.
- Harris, D. V., Matias, L., Thomas, L., Harwood, J., and Geissler, W. H. (2013). "Applying distance sampling to fin whale calls recorded by single seismic instruments in the northeast Atlantic," *J. Acoust. Soc. Am.* **134**, 3522–3535.
- Harris, D. V., Miksis-Olds, J. L., Vernon, J. A., and Thomas, L. (2018). "Fin whale density and distribution estimation using acoustic bearings derived from sparse arrays," *J. Acoust. Soc. Am.* **143**, 2980–2993.
- Helble, T. A., D'Spain, G. L., Hildebrand, J. A., Campbell, G. S., Campbell, R. L., and Heaney, K. D. (2013). "Site specific probability of passive acoustic detection of humpback whale calls from single fixed hydrophones," *J. Acoust. Soc. Am.* **134**, 2556–2570.
- Helble, T. A., Ierley, G. R., D'Spain, G. L., and Martin, S. W. (2015). "Automated acoustic localization and call association for vocalizing humpback whales on the Navy's Pacific Missile Range Facility," *J. Acoust. Soc. Am.* **137**, 11–21.
- Hendricks, B., Keen, E. M., Shine, C., Wray, J. L., Alidina, H. M., and Picard, C. R. (2021). "Acoustic tracking of fin whales: Habitat use and movement patterns within a Canadian Pacific fjord system," *J. Acoust. Soc. Am.* **149**, 4264–4280.
- Ierley, G., and Helble, T. A. (2016). "Fin whale call sequence analysis from tracked fin whales on the Southern California Offshore Range," *J. Acoust. Soc. Am.* **140**, 3295.
- Jarvis, S. M., Morrissey, R. P., Moretti, D. J., DiMarzio, N. A., and Shaffer, J. A. (2014). "Marine Mammal Monitoring on Navy Ranges (M3R): A toolset for automated detection, localization, and monitoring of marine mammals in open ocean environments," *Mar. Technol. Soc. J.* **48**, 5–20.
- Johnson, M. P., and Tyack, P. L. (2003). "A digital acoustic recording tag for measuring the response of wild marine mammals to sound," *IEEE J. Oceanic Eng.* **28**, 3–12.
- Klinck, H., Fregosi, S., Matsumoto, H., Turpin, A., Mellinger, D. K., Erofeev, A., Barth, J. A., Shearman, R. K., Jafarmadar, K., and Stelzer, R. (2016). "Mobile autonomous platforms for passive-acoustic monitoring of high-frequency cetaceans," in *Robot. Sail*, edited by A. Friebe and F. Haug (Springer, Cham, Switzerland), pp. 29–37.
- Kowarski, K. A., Gaudet, B. J., Cole, A. J., Maxner, E. E., Turner, S. P., Martin, S. B., Johnson, H. D., and Moloney, J. E. (2020). "Near real-time marine mammal monitoring from gliders: Practical challenges, system development, and management implications," *J. Acoust. Soc. Am.* **148**, 1215–1230.
- Küsel, E. T., Munoz, T., Siderius, M., Mellinger, D. K., and Heimlich, S. (2017). "Marine mammal tracks from two-hydrophone acoustic recordings made with a glider," *Ocean Sci.* **13**, 273–288.
- Kyhn, L. A., Tougaard, J., Thomas, L., Duve, L. R., Stenback, J., Amundin, M., Desportes, G., and Teilmann, J. (2012). "From echolocation clicks to animal density—Acoustic sampling of harbor porpoises with static dataloggers," *J. Acoust. Soc. Am.* **131**, 550–560.
- Marques, T. A., Munger, L., Thomas, L., Wiggins, S., and Hildebrand, J. A. (2011). "Estimating North Pacific right whale *Eubalaena japonica* density using passive acoustic cue counting," *Endang. Species Res.* **13**, 163–172.
- Marques, T. A., Thomas, L., Martin, S. W., Mellinger, D. K., Ward, J. A., Moretti, D. J., Harris, D. V., and Tyack, P. L. (2013). "Estimating animal population density using passive acoustics," *Biol. Rev.* **88**, 287–309.
- Marques, T. A., Thomas, L., Ward, J., DiMarzio, N., and Tyack, P. L. (2009). "Estimating cetacean population density using fixed passive acoustic sensors: An example with Blainville's beaked whales," *J. Acoust. Soc. Am.* **125**, 1982–1994.
- Martin, S. W., Martin, C. R., Matsuyama, B. M., and Henderson, E. E. (2015). "Minke whales (*Balaenoptera acutorostrata*) respond to navy training," *J. Acoust. Soc. Am.* **137**, 2533–2541.
- Martin, S. W., and Matsuyama, B. (2015). "Suspected Bryde's whales acoustically detected, localized and tracked using recorded data from the Pacific Missile Range Facility, Hawaii," [https://www.navy.marin-species-monitoring.us/files/7114/3826/9215/Martin\\_and\\_Matsuyama\\_2015\\_Suspected\\_Brydes\\_detected\\_at\\_PMRF\\_20JUL2015.pdf](https://www.navy.marin-species-monitoring.us/files/7114/3826/9215/Martin_and_Matsuyama_2015_Suspected_Brydes_detected_at_PMRF_20JUL2015.pdf) (Last viewed 6/12/2020).
- Matsumoto, H., Haxel, J., Turpin, A., Fregosi, S., Klinck, H., Klinck, K., Baumann-Pickering, S., Erofeev, A., Barth, J. A., Dziak, R. P., and Jones, C. (2015). "Simultaneous operation of mobile acoustic recording systems off the Washington Coast for cetacean studies: System noise level evaluations," in *Proceedings of OCEANS 2015—MTS/IEEE Washington*, October 19–22, Washington, DC.
- McDonald, M. A., and Fox, C. G. (1999). "Passive acoustic methods applied to fin whale population density estimation," *J. Acoust. Soc. Am.* **105**, 2643–2651.
- McDonald, M. A., Hildebrand, J. A., and Webb, S. C. (1995). "Blue and fin whales observed on a seafloor array in the Northeast Pacific," *J. Acoust. Soc. Am.* **98**, 712–721.
- Moretti, D., Marques, T. A., Thomas, L., DiMarzio, N., Dilley, A., Morrissey, R., McCarthy, E., Ward, J., and Jarvis, S. (2010). "A dive counting density estimation method for Blainville's beaked whale (*Mesoplodon densirostris*) using a bottom-mounted hydrophone field as applied to a mid-frequency active (MFA) sonar operation," *Appl. Acoust.* **71**, 1036–1042.
- Moretti, D., Morrissey, R., Jarvis, S., and Shaffer, J. (2016). "Findings from U.S. Navy hydrophone ranges," in *Listening in the Ocean*, edited by W. W. L. Au and M. O. Lammers (Springer, New York), pp. 239–256.
- Norris, T. F., Dunleavy, K. J., Yack, T. M., and Ferguson, E. L. (2017). "Estimation of minke whale abundance from an acoustic line transect survey of the Mariana Islands," *Mar. Mam. Sci.* **33**, 574–592.
- Oleson, E. M., Širović, A., Bayless, A. R., and Hildebrand, J. A. (2014). "Synchronous seasonal change in fin whale song in the North Pacific," *PLoS One* **9**, e115678.
- R Core Team (2019). *R: A Language and Environment for Statistical Computing* (R Foundation for Statistical Computing, Vienna, Austria).
- Rudnick, D. L., Davis, R. E., Eriksen, C. C., Fratantoni, D. M., and Perry, M. J. (2004). "Underwater gliders for ocean research," *Mar. Technol. Soc. J.* **38**, 73–84.
- Sato, K., Watanuki, Y., Takahashi, A., Miller, P. J. O., Tanaka, H., Kawabe, R., Ponganis, P. J., Handrich, Y., Akamatsu, T., Watanabe, Y., Mitani, Y., Costa, D. P., Bost, C. A., Aoki, K., Amano, M., Trathan, P., Shapiro, A., and Naito, Y. (2007). "Stroke frequency, but not swimming speed, is related to body size in free-ranging seabirds, pinnipeds and cetaceans," *Proc. Biol. Sci.* **274**, 471–477.
- Seber, G. A. F. (1982). *The Estimation of Animal Abundance and Related Parameters*, 2nd ed. (Griffin, London).
- Silva, T., Mooney, T., Sayigh, L., and Baumgartner, M. (2019). "Temporal and spatial distributions of delphinid species in Massachusetts Bay using passive acoustics from ocean gliders," *Mar. Ecol. Prog. Ser.* **631**, 1–17.
- Širović, A., Hildebrand, J. A., and Wiggins, S. M. (2007). "Blue and fin whale call source levels and propagation range in the Southern Ocean," *J. Acoust. Soc. Am.* **122**, 1208–1215.
- Širović, A., Oleson, E. M., Buccowich, J., Rice, A., and Bayless, A. (2017). "Fin whale song variability in southern California and the Gulf of California," *Sci. Rep.* **7**, 10126.
- Širović, A., Rice, A., Chou, E., Hildebrand, J. A., Wiggins, S. M., and Roch, M. A. (2015). "Seven years of blue and fin whale call abundance in the Southern California Bight," *Endang. Species Res.* **28**, 61–76.
- Širović, A., Williams, L., Kerosky, S., Wiggins, S., and Hildebrand, J. (2013). "Temporal separation of two fin whale call types across the eastern North Pacific," *Mar. Biol.* **160**, 47–57.



- Soule, D. C., and Wilcock, W. S. D. (2013). "Fin whale tracks recorded by a seismic network on the Juan de Fuca Ridge, Northeast Pacific Ocean," *J. Acoust. Soc. Am.* **133**, 1751–1762.
- Stafford, K. M., Mellinger, D. K., Moore, S. E., and Fox, C. G. (2007). "Seasonal variability and detection range modeling of baleen whale calls in the Gulf of Alaska, 1999–2002," *J. Acoust. Soc. Am.* **122**, 3378–3390.
- Stimpert, A. K., DeRuiter, S. L., Flacone, E. A., Joseph, J., Douglas, A. B., Moretti, D. J., Friedlaender, A. S., Calambokidis, J., Gailey, G., Tyack, P. L., and Goldbogen, J. A. (2015). "Sound production and associated behavior of tagged fin whales (*Balaenoptera physalus*) in the Southern California Bight," *Anim. Biotelemetry* **3**, 23.
- Thompson, P. O., Findley, L. T., and Vidal, O. (1992). "20-Hz pulses and other vocalizations of fin whales, *Balaenoptera physalus*, in the Gulf of California, Mexico," *J. Acoust. Soc. Am.* **92**, 3051–3057.
- Thompson, P. O., and Friedl, W. A. (1982). "A long term study of low frequency sounds from several species of whales off Oahu, Hawaii," *Cetology* **45**, 1–19.
- University of Washington (2016). "Seaglider quality control manual," [https://gliderfs2.coas.oregonstate.edu/sgliderweb/Seaglider\\_Quality\\_Control\\_Manual.html](https://gliderfs2.coas.oregonstate.edu/sgliderweb/Seaglider_Quality_Control_Manual.html) (Last viewed 10/12/2022).
- Urick, R. (1983). *Principles of Underwater Sound*, 3rd ed. (Peninsula, Los Altos, CA).
- Verfuss, U. K., Aniceto, A. S., Harris, D. V., Gillespie, D., Fielding, S., Jiménez, G., Johnston, P., Sinclair, R. R., Sivertsen, A., Solbø, S. A., Storvold, R., Biuw, M., and Wyatt, R. (2019). "A review of unmanned vehicles for the detection and monitoring of marine fauna," *Mar. Pollut. Bull.* **140**, 17–29.
- Ward, J. A., Jarvis, S., Moretti, D. J., Morrissey, R. P., Dimarzio, N., Johnson, M. P., Tyack, P. L., Thomas, L., and Marques, T. A. (2011). "Beaked whale (*Mesoplodon densirostris*) passive acoustic detection in increasing ambient noise," *J. Acoust. Soc. Am.* **129**, 662–669.
- Ward, J. A., Thomas, L., Jarvis, S., Dimarzio, N., Moretti, D., Marques, T. A., Dunn, C., C laridge, D., Hartvig, E., and Tyack, P. (2012). "Passive acoustic density estimation of sperm whales in the Tongue of the Ocean, Bahamas," *Mar. Mamm. Sci.* **28**, E444–E455.
- Watkins, W. A. (1981). "Activities and underwater sounds of fin whales," *Sci. Rep. Whales Res. Inst.* **33**, 83–117.
- Watkins, W. A., Daher, M. A., Reppucci, G. M., George, J. E., Martin, N. A., Dimarzio, N. A., and Gannon, D. P. (2000). "Seasonality and distribution of whale calls in the North Pacific," *Oceanography* **13**, 62–67.
- Watkins, W. A., Tyack, P., Moore, K. E., and Bird, J. E. (1987). "The 20-Hz signals of finback whales (*Balaenoptera physalus*)," *J. Acoust. Soc. Am.* **82**, 1901–1912.
- Wood, S., and Scheipl, F. (2017). "gamm4: Generalized additive mixed models using 'mgcv' and 'lme4,'" <https://rdrr.io/cran/gamm4/man/gamm4.html> (Last viewed 10/12/2022).
- Wood, S. N. (2017). *Generalized Additive Models: An Introduction with R* (CRC, Boca Raton, FL).